

Optofluidic gradient refractive index resonators using liquid diffusion for tunable unidirectional emission

Electronic Supplementary Information

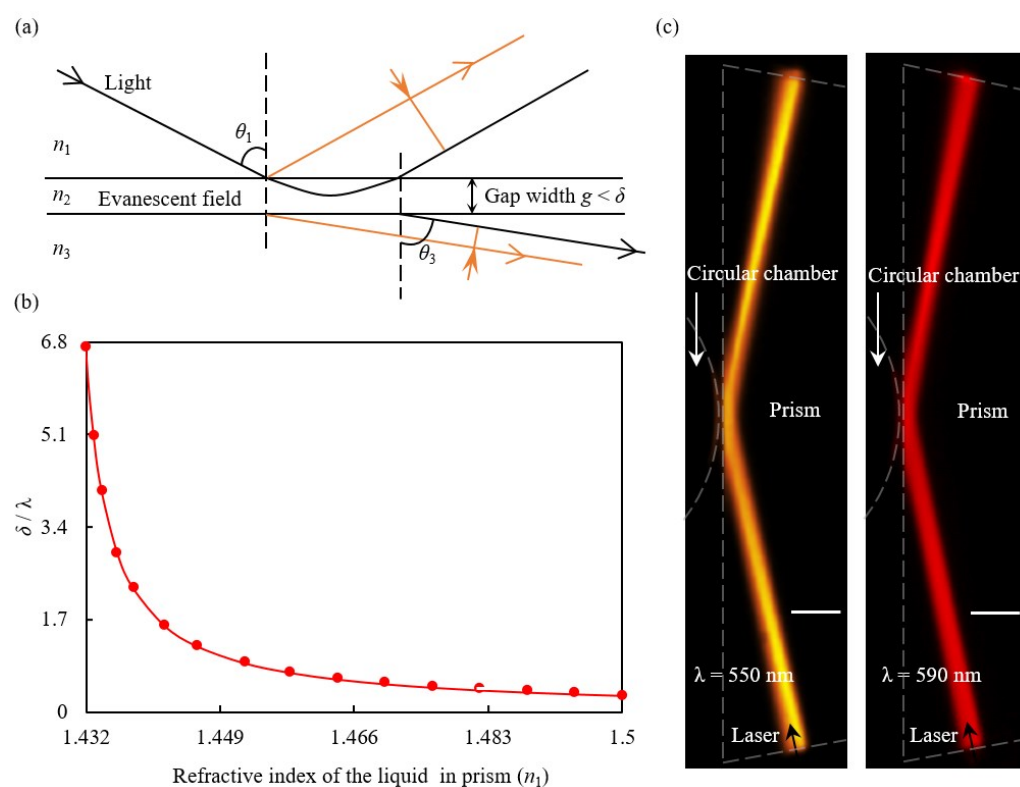


Fig. S1 Coupling between the prism and gradient-index resonator. (a) Total internal reflection for coupling process. Here, $\theta_1 = 79.5^\circ$; gap width $g = 600$ nm (the shortest distance between the prism and resonator); n_1 , n_2 , and n_3 are the refractive indices of the prism, PDMS (1.405) and ethylene glycol (1.432). To ensure total internal reflection, $n_1 > n_2/\sin\theta_1 = 1.429$. When $g < \delta$, $n_1\sin\theta_1 = n_3\sin\theta_3$. Solid black arrows represent the light path while the orange arrows show the light displacement caused by total internal reflection. (b) The fraction δ/λ (where λ is wavelength) as a function of the refractive index of the liquid in prism. The value of δ can be modulated by the refractive-index difference, $n_1 - n_2$. (c) Experimental total internal reflection for incident wavelengths of 550 and 590 nm. The scale bars represent 20 μm .

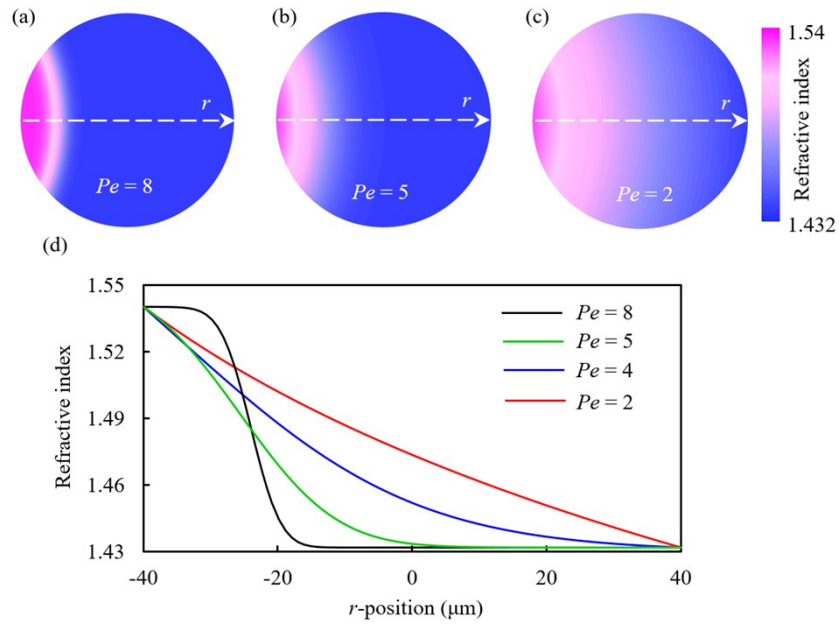


Fig. S2 Dependence of refractive index distribution on flow rates (Pe) for $R = 100 \mu\text{m}$. (a)-(c) Refractive-index profiles at $Pe = 8, 5$ and 2 , respectively. (d) Refractive index on r axis. When the flow rates are low enough such as $Pe = 2$, the diffusion is complete to form gradient-index profile.

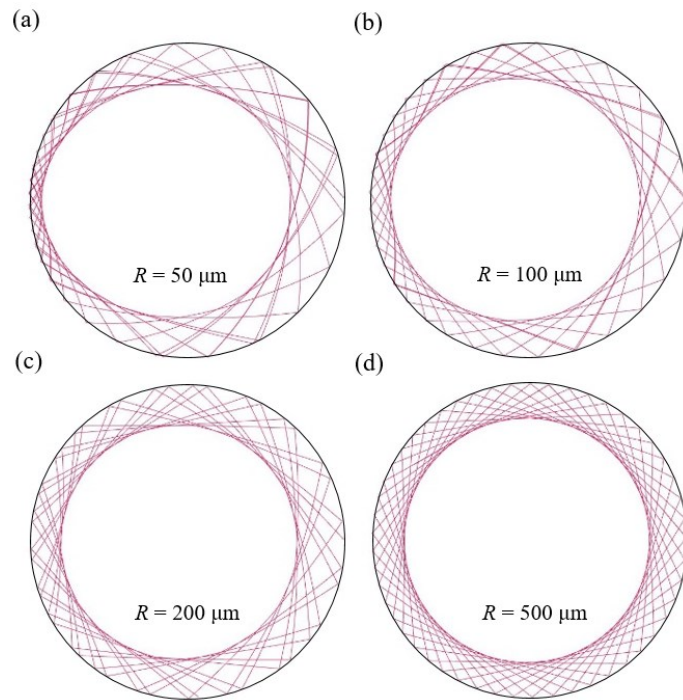


Fig. S3 (a)-(d) Simulated ray trajectory for different bending radii. It clearly shows that the “squeezing” of light is pronounced for smaller bending radius. When the bending radius is larger enough such as $R = 500 \mu\text{m}$, the special squeezed performance disappears, meaning that this gradient-index resonator loses its characteristics.

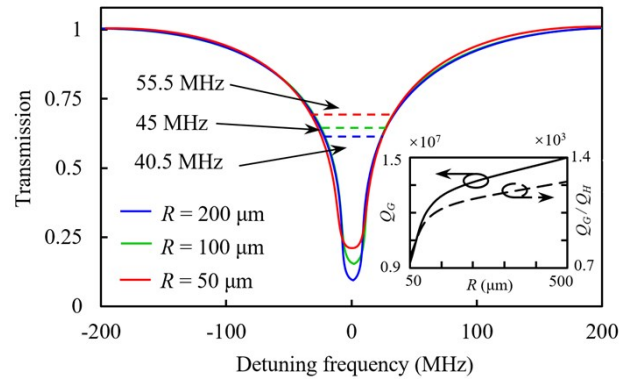


Fig. S4 Simulated transmission spectra at incident wavelength of 550 nm. According to the formula $Q = f / \Delta f$, where f is the resonant frequency and Δf is the bandwidth, we can obtain the quality factor is on the order of 10^7 . In details, the bandwidth is relatively smaller as R increases, resulting in higher quality factor for large bending radii R , which may be caused by the reduction of the squeezing of high refractive-index region or light prolife. Inset shows the dependence of quality factor on bending radii. Q_G is for this gradient-index resonator and Q_H is for homogeneous counterparts, showing nearly one thousand times higher of this resonator than conventional models.

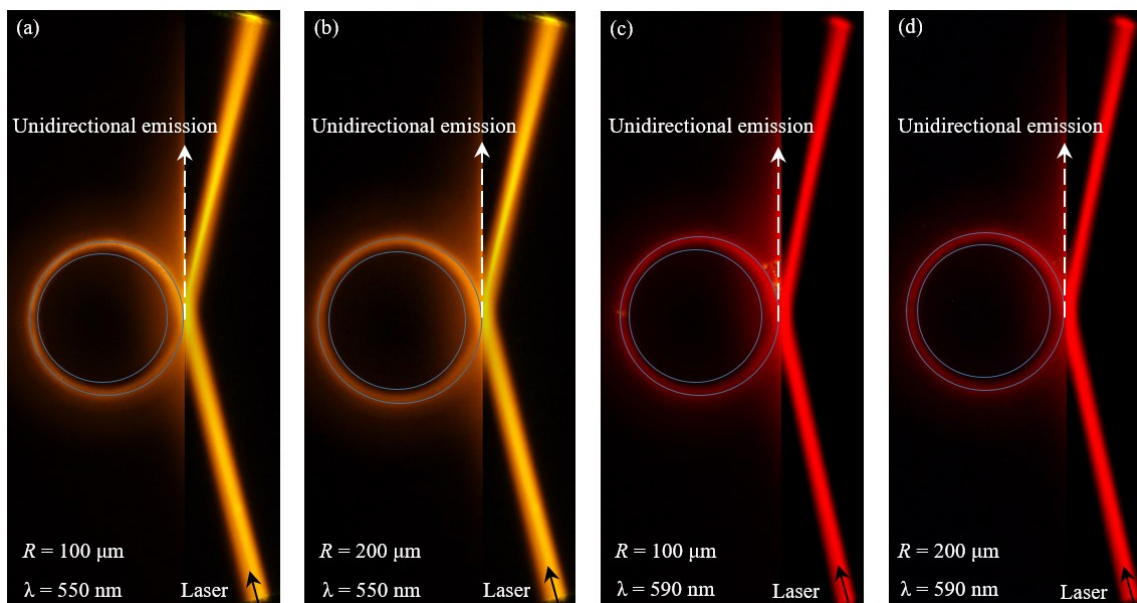


Fig. S5 Light propagation for different bending radii R and incident wavelengths λ . The liquids in the resonator (left side of each figure) and prism (right side of each figure) are both dyed with Rhodamine 640 to visualise the light. The green and red filters are used to filter out excitation light of wavelengths 550 and 590 nm, respectively. (a), (b) Optical resonance at 550 nm for $R = 100$ and $200 \mu\text{m}$, respectively. (c), (d) Optical resonance at 590 nm for $R = 100$ and $200 \mu\text{m}$, respectively.